JOURNAL OF MATERIALS SCIENCE 10 (1975) 365–378

Condensation of cadmium aerosols

E. R. BUCKLE, K. C. POINTON
Department of Metallurgy, The University, Sheffield, UK

Cadmium aerosols were prepared by the heat-pulse method and fall-out collected at temperatures T from ambient to just above the melting point T_f. Deposits were examined by electron microscopy after coating with Au–Pd. Representative particles were removed for electron and X-ray diffraction studies.

The particles are crystalline. The types, and their proportions and size distributions vary with temperature. At low temperatures particles are monocrystals of high specific surface, chiefly prisms with deep fissures and cavities but also rough spheres and stellate dendrites. At higher temperatures the crystal forms are perfected, the proportion of prisms falls, and polycrystalline as well as monocrystalline spheres are found. Spheres can exceed 50μm in diameter but the largest prisms are 2 to 3 μm and disappear at 0.8 to 0.9 T_f. Up to this point spheres have one or more circular {0001} depressions, or "dishes", depending on the number of crystallites they contain. At higher temperatures they are quite smooth.

It is concluded that smooth spheres are droplets which have supercooled and frozen on the collector, and as such are not aerosol particles. Droplets that freeze in the cloud become dished spheres, and their subsequent growth involves condensation on areas between the dishes. All particles are nucleated from the vapour close to the source, the prisms apparently at $T < T_f$.

1. Introduction

A batch method for studying the condensation of metallic aerosols from the vapour in the presence of purified argon was recently described [1]. Supersaturated metal vapour is generated by flash-heating a small metal sample in a furnace held at a steady background temperature, T. As the vapour cools it condenses to an aerosol of liquid or solid particles depending on the temperature. The growth and evaporation of the cloud particles is studied while they are in motion by watching the Airy patterns through a telescope. By repeating the condensation while slowly varying T, the temperature-sensitive properties of aerosols may be investigated.

The apparatus was described previously [1] but the results given were of a preliminary nature and restricted to telescopic observations. The cloud chamber and experimental technique have since been improved to allow particles deposited from the clouds to be collected without deterioration for examination by electron microscopy and by electron and X-ray diffraction. These modifications are now described together with the results of a detailed study of Cd. The types of particle are first classified according to shape and crystallinity. An attempt is then made to relate the types to the operating conditions that lead to their formation.

2. Experimental

Cadmium wire (Metals Research, Ltd, 99.9999% pure) was used as the vapour source. Aerosols were generated as previously [1] at a series of temperatures up to 594 K, which is 31 K above the melting point, T_f.

2.1. Protection of particles from the atmosphere

Particles from condensation aerosols have often been shown to be abnormally reactive. In the case of metals they are even pyrophoric. Gen *et al.* [2] found that Al powders would sometimes ignite spontaneously when exposed to air. Condensates of several metals were examined after exposure to air by Kimoto and associates [3, 4] and oxidation confirmed by the diffraction patterns in the electron microscope. Such contamination can obliterate the original habit of a condensed particle, and it was considered

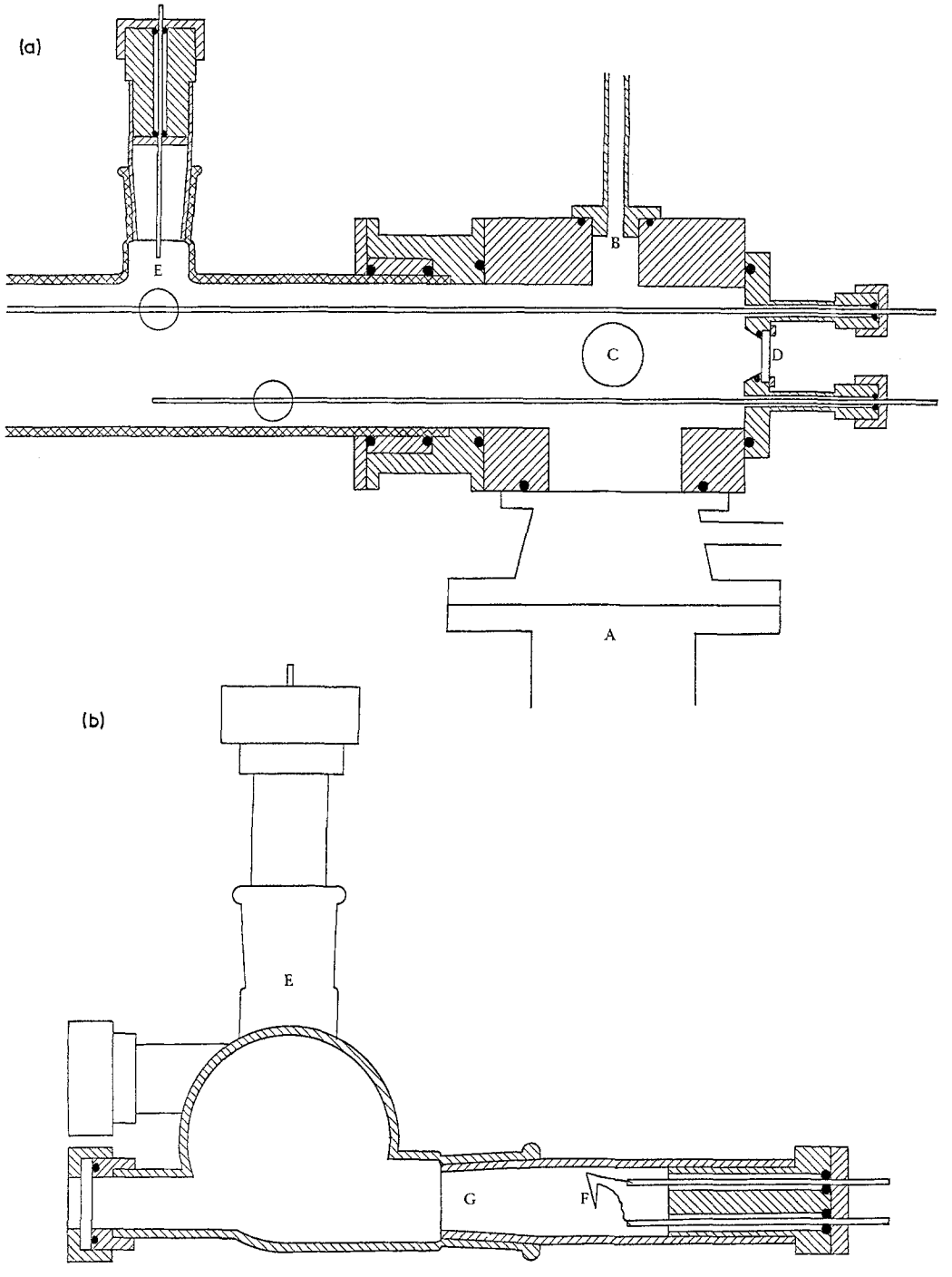

Figure 1 Manipulation end of cloud chamber. (a) Longitudinal section: A, diffusion pump; B, Ar inlet; C, Penning gauge; D, chamber observation window; E, supersaturator access turret. (b) Radial section: F, heating filament; G, substrate access turret.

essential in the present work to protect the fall-out with a thin layer of inert metal.

A protective coat of 60% Au–40% Pd was applied over the specimen by vacuum evapora-

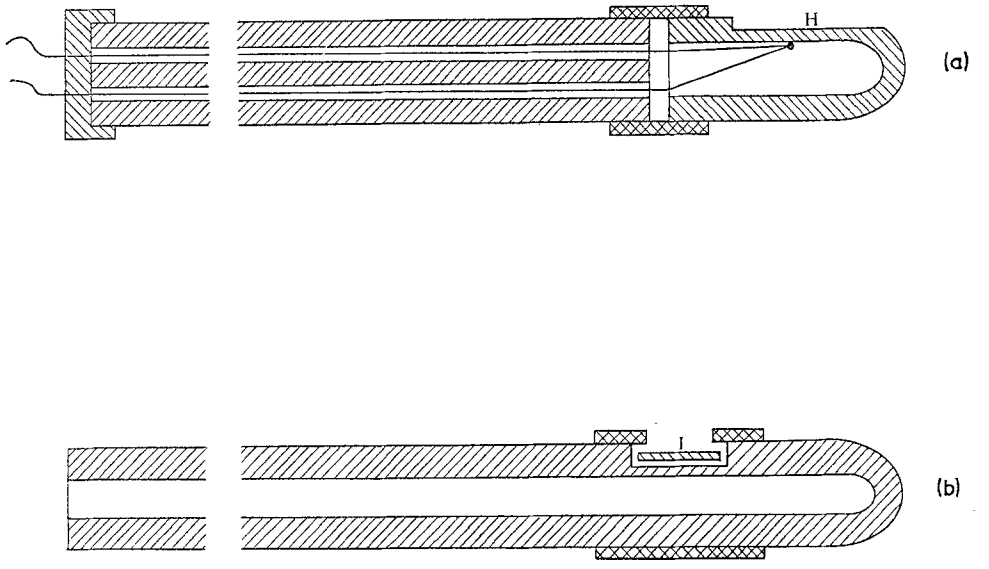

Figure 2 Substrate probe for (a) scanning electron microscopy, (b) transmission electron microscopy. H, silica substrate; I, Au grid.

tion. To achieve a reliable technique a modification to the cloud chamber was necessary. The head mounted at the manipulation end was altered to allow direct connection to a 2-inch silicone-oil diffusion pump so as to achieve pressures below 10^{-4} Torr (Fig. 1a).

The heating filament was a V-shaped loop of W wire of 0.5 mm diameter mounted on thick Cu electrodes and inserted into the substrate access turret (Fig. 1b). The filament was supplied with current from the supersaturator supply. Au–Pd wire of 0.25 mm diameter was wound round the apex of the filament, the amount of wire and the distance to the substrate being adjusted to give a film 10 nm thick on the assumption that the emission from the source was spherically symmetrical [5]. The substrate was rotated and oscillated during evaporation to promote good coverage.

2.2. Scanning electron microscopy

For study by scanning electron microscopy aerosols were sampled by allowing them to settle on a horizontal flat of polished silica. The flat was attached to the substrate probe with a sleeve of Pt–Rh foil (Fig. 2a). The thermocouple in the probe gave an approximate reading of the temperature of the silica surface.

2.3. Transmission electron microscopy

Particles were collected for transmission electron microscopy on a carbon membrane some 40 nm thick supported on a 200-mesh grid of Au. The grid fitted into a recess in the substrate probe and was held in place by a tightly-fitting sleeve of Pt–Rh (Fig. 2b). Preparation of a membrane thin enough for electron beam penetration but strong enough to support the particles and withstand the temperature and necessary manipulation inside the cloud chamber involved some difficulty. In the procedure finally adopted a microscope slide was cleaned with detergent and polished dry with a soft cloth without rinsing. The hydrophilic layer left on the glass facilitated the later removal of the carbon membrane. This was deposited by striking an arc between two pointed graphite rods under a vacuum of better than 10^{-3} Torr. With the slide 10 to 15 cm from the arc and a current of 50 A sufficient material was deposited in about 0.5 sec. Squares of membrane were transferred by flotation to grids coated with polybutene from a 1 % solution in xylene. This proved effective in preventing detachment [6].

2.4. X-ray diffraction

X-ray diffraction was used to examine the crystallinity of particles too thick for penetration by electrons in the 1 MV microscope. Selected particles were plucked from the sample under a stereo-microscope with the greased tip of a

fine glass fibre. Back-reflection Läue photographs were taken with a 100 μm beam from a Cu target.

3. Results

3.1. Particle morphology

The particles observed in the fall-out were prisms and spheroids with a variety of surface features. We list first the particles according to their images in the scanning electron microscope (Table I). Their descriptions refer to their aspects after settling and coating. A particle was distinguished as a type for this purpose if it seemed on cursory examination that it might have had a separate origin in the chamber or been an artefact of the sedimentary process. Further information was then obtained by selecting particles for individual examination. This enabled the types of Table I to be interrelated and classified with greater brevity in the form of Table II.

TABLE I Types of particles in fall-out

Description	Figure
Prisms	
(a) Simple prism	3a, b
(b) Dendrite	3c
(c) Prism with pyramidal faces	3d
Spheroids	
(d) Dished sphere with orientated facets	4a
(e) Tree-ringed sphere with orientated facets	4b
(f) Dished sphere	4e
(g) Multi-dished sphere	5a
(h) Polyhedron with several unrelated faces	5b
(i) Multi-facetted sphere	5c
(j) Combined spheres	5d
(k) Smooth sphere	10a

TABLE II Classification of aerosol particles

Description	Types included (Table I)	Crystallinity
Simple prism	(a)	mono
Dendrite	(b)	—
Pyramidal prism	(c)	mono
Spherical monocrystal	(d, e, f)	mono
Spherical polycrystal	(g, h, i, k*)	poly

*Crystallize after sedimentation.

The sequence (a) to (k) in Table I gives roughly the succession in the fall-out as the temperature was increased from 0.49 T_f to 1.05 T_f. Electron micrographs of the main types are given in Figs. 3 to 5 and morphological charts in Fig. 6. The charts show how the size of a particle of a given type (abscissa) and its fraction in the fall-out (linewidth) varied with temperature (ordinate). Population fractions are only qualitative but the charts are valuable in the interpretation of the sequence (a) to (k).

The prisms had a narrow size range and rarely exceeded 2 μm in diameter. They were shown by electron diffraction (AEI EM7 Microscope) to be monocrystals. With the temperature at room level the simple prisms were for the most part poorly developed, the hexagonal faces on each side being deeply pitted as though etched (Fig. 3b). Dendrites were also present but these were considerably larger and rarer (Fig. 3c). The three-dimensional, stellate form resembles that of dendrites seen in certain salt aerosols [7]. As the temperature was raised the faces of simple prisms tended to become smoother (Fig. 3a) but eventually the simple habit gave way to a pyramidal one (Fig. 3d). Prisms vanished altogether when the temperature exceeded $\sim 0.9\ T_f$.

An outstanding feature of the spheroidal particles which condensed at $T < T_f$ was the presence of one or more "dishes" (Figs. 4 and 5). A dish is a shallow circular depression, the concavity having been verified from stereo pairs taken with the scanning electron microscope. A second important characteristic of singly-dished spheres was the presence of "tree rings" (Fig. 4). The rings are formed by concentric growth ledges spread over the convex area of the surface. After repeated examination of many fields it was concluded that the centre of the rings always lies on the surface at a point diametrically opposite the centre of a dish, so that particles with one dish and particles with a set of tree rings are identical species (Table I, d, e). This is verified by the identity of the size-ranges (Fig. 6).

The other notable feature of the dished and tree-ringed sphere was the regular array of facets and rough intermediate regions outside the dish. The symmetry suggested that the particles were crystalline, possibly monocrystals, and this was confirmed by electron diffraction. The polyhedral shape conferred by the facets was at its clearest in room-temperature fall-out but it was at 0.6 T_f to 0.8 T_f that such particles were most abundant.

The shape of these spherical monocrystals became rounder and smoother at higher temperatures although the dish was always present (Fig. 4). The ultimate form appeared to

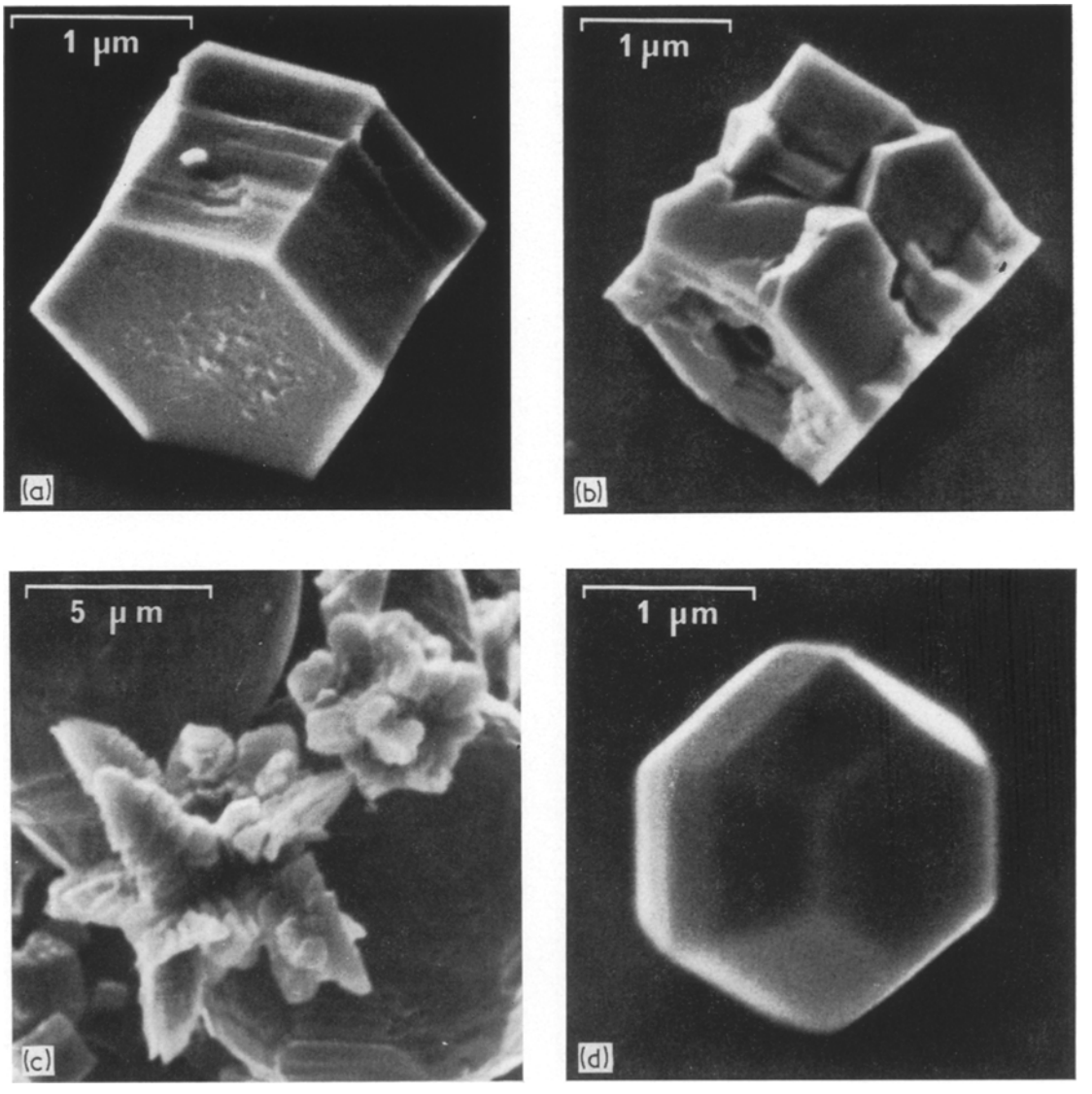

Figure 3 Prismatic crystals. (a) Simple prism, (b) cavitated Simple prism, (c) dendrite, (d) prism with pyramidal faces.

be the dished sphere (Table I, f). This type became more prevalent as the temperature was raised, and apart from the dish it had no recognizable surface structure (Fig. 4e). X-ray diffraction showed dished spheres to be monocrystalline also, and the three types (d), (e) and (f) of Table I are classified together as spherical monocrystals in Table II.

Other spherical forms were present over most of the range below 0.8 T_f. These particles (Table I, g, h) did not show tree rings and were either spheres with several dishes (Fig. 5a) or polyhedra with several prominent faces in apparently unrelated orientations (Fig. 5b). Polyhedra were larger on the whole than multi-dished spheres, and both were larger and more uniform in size than the spherical monocrystals (Fig. 6). The Läue patterns of the single particles could not be indexed but the multiplication of spots suggested that they were composed of at least three crystallites. Grooves were sometimes visible between the faces of the polyhedra (Fig. 7) and it would be in keeping with the polycrystalline nature of the particles to identify them

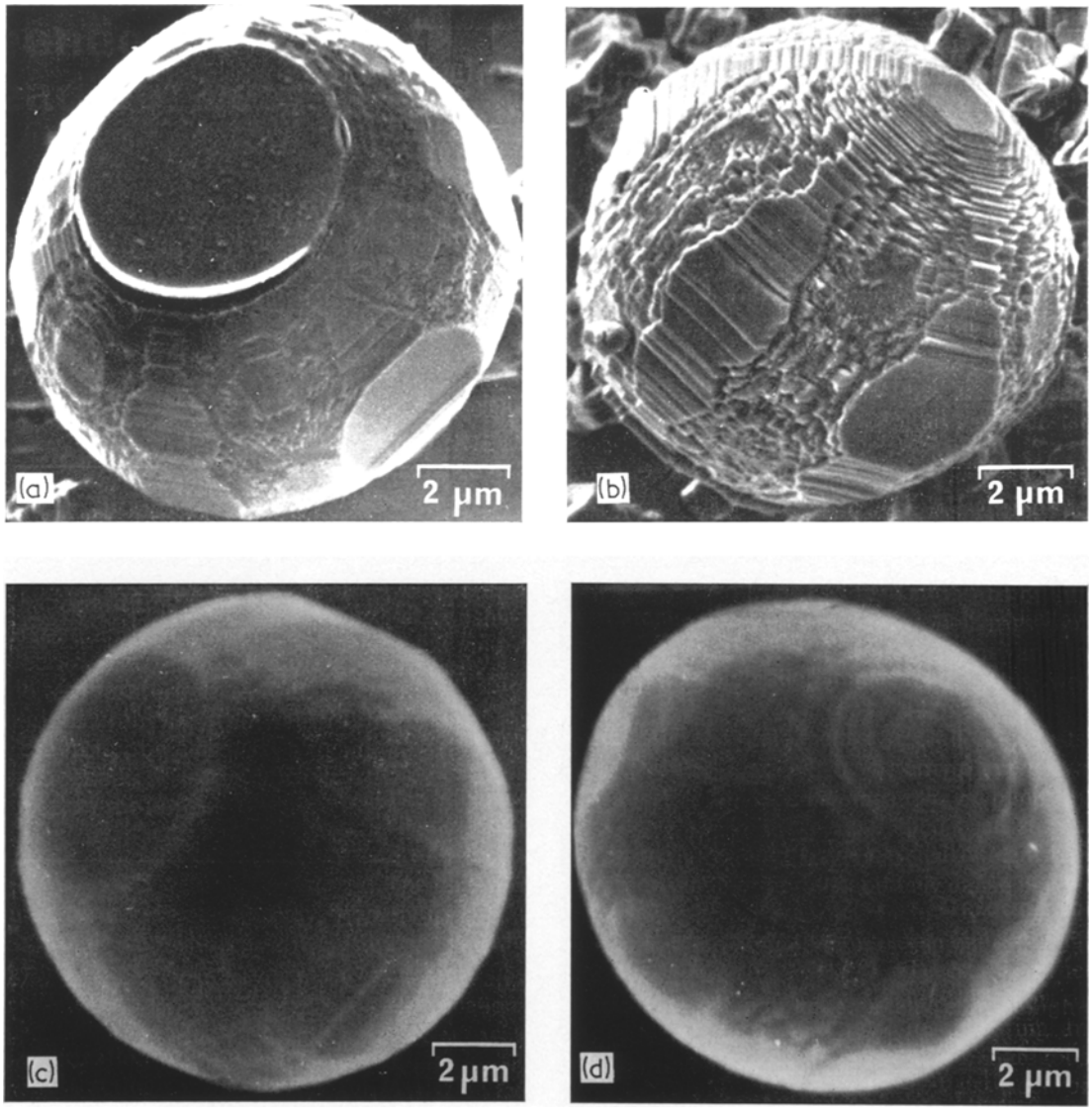

Figure 4.

with grain boundaries. Cases were also seen where the grooves divided a dish into two roughly equal parts, suggestive of nucleation twinning.

Above 0.8 T_f these particles were succeeded by polyhedra with very many faces (Table I, i). Fig. 6 shows that these were essentially a high-temperature form of wide-ranging size but comparatively rare. Läue patterns again indicated several crystallites per particle. Fig. 8 shows one such particle in which damage had by chance made visible the interior. The impression gained is that the surface facets were the result of so-called "parasitic nucleation" [8] of a polycrystalline Cd layer on a Cd sphere, but there were no rings in the Laue pattern to support this.

Many particles in fall-out above 0.8 T_f were composite. They appear to have resulted from the sintering of single particles because the spherical form and even dishes of the component particles often remain evident (Fig. 5d). Only one example was seen of a flat particle. This resembled a splashed droplet (Fig. 9) and occurred in a sample taken at 0.85 T_f. Both kinds of particle, sintered and splashed, are believed to

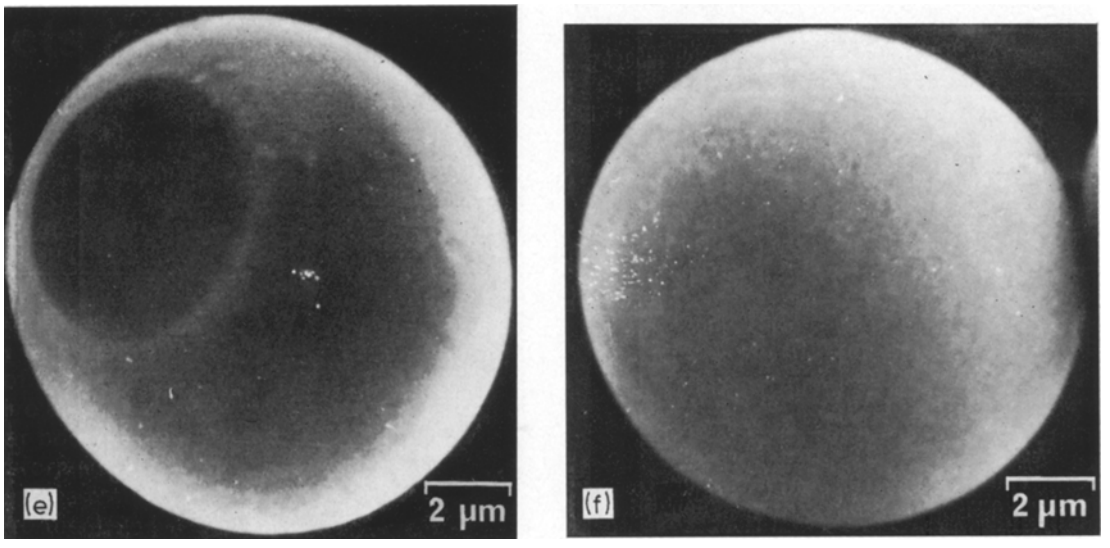

Figure 4 Spherical monocrystals (front and back views). (a) and (b) dished and tree-ringed sphere at 0.49 T_f; (c) and (d) dished and tree-ringed sphere at 0.76 T_f; (e) and(f) dished sphere at 0.85 T_f.

have taken the form observed after impact of the metal with the substrate, and for this reason they are not classified as aerosol particles in Table II. That splashing was not general even above T_f is attributed to the low impact velocities of the descending particles, and the isolated example of Fig. 9 may have been a large drop of molten metal from the supersaturator.

Smooth spheres (Table I, k) occurred in the trans-T_f region of temperature and are so called because in the as-deposited condition only minor surface features or departures from sphericity were detectable (Fig. 10a). Detachment from the substrate occasionally revealed a slight flattening at the point of contact but there were no dishes. X-ray diffraction on particles of sufficient size (50 μm) showed the smooth spheres also to be composed of three or more individual crystals. Faint arcs through the spots were also visible in this case and were possibly produced by many very small Cd crystallites in random or slightly-preferred orientations. It was also noticeable that smooth spheres were frequently contaminated with amorphous material, possibly oxide, at points on the surface, particularly where the protective covering of Au–Pd was incomplete. A particle badly contaminated by atmospheric exposure is shown in Fig. 10b. For simplicity, the smooth spheres are classified with the other polycrystals in Table II under the description "spherical polycrystals", although those which are condensed at $T > T_f$ cannot solidify in the cloud.

3.2. Distribution of fall-out over substrate

To ascertain that the fall-out was uniform along the chamber axis a substrate was exposed to several cloudbursts at 0.76 T_f and examined extensively in the electron microscope. Counts of the total number of particles were made over several fields along the specimen in the direction of the chamber axis. The counts were substantially the same. This confirms that the total concentration of particles in the aerosol is homogeneous, as might be expected from the uniform toroidal motion it adopts before the vapour supply is cut off [1]. The size distribution, irrespective of particle type, was also counted and found to be constant and lognormal. A curve derived for a count of 6000 particles is given in Fig. 11, where D is the particle diameter (μm) and f_D is the fraction of particles with sizes up to D.

4. Discussion

Our present method of observing particles while in suspension reveals only the motion and brightness of their Airy patterns as seen in the telescope. The methods used to detect the solidification event in molten salt aerosols [7] have so far been unsuccessful with metals [1]. All the particles examined by electron and X-ray

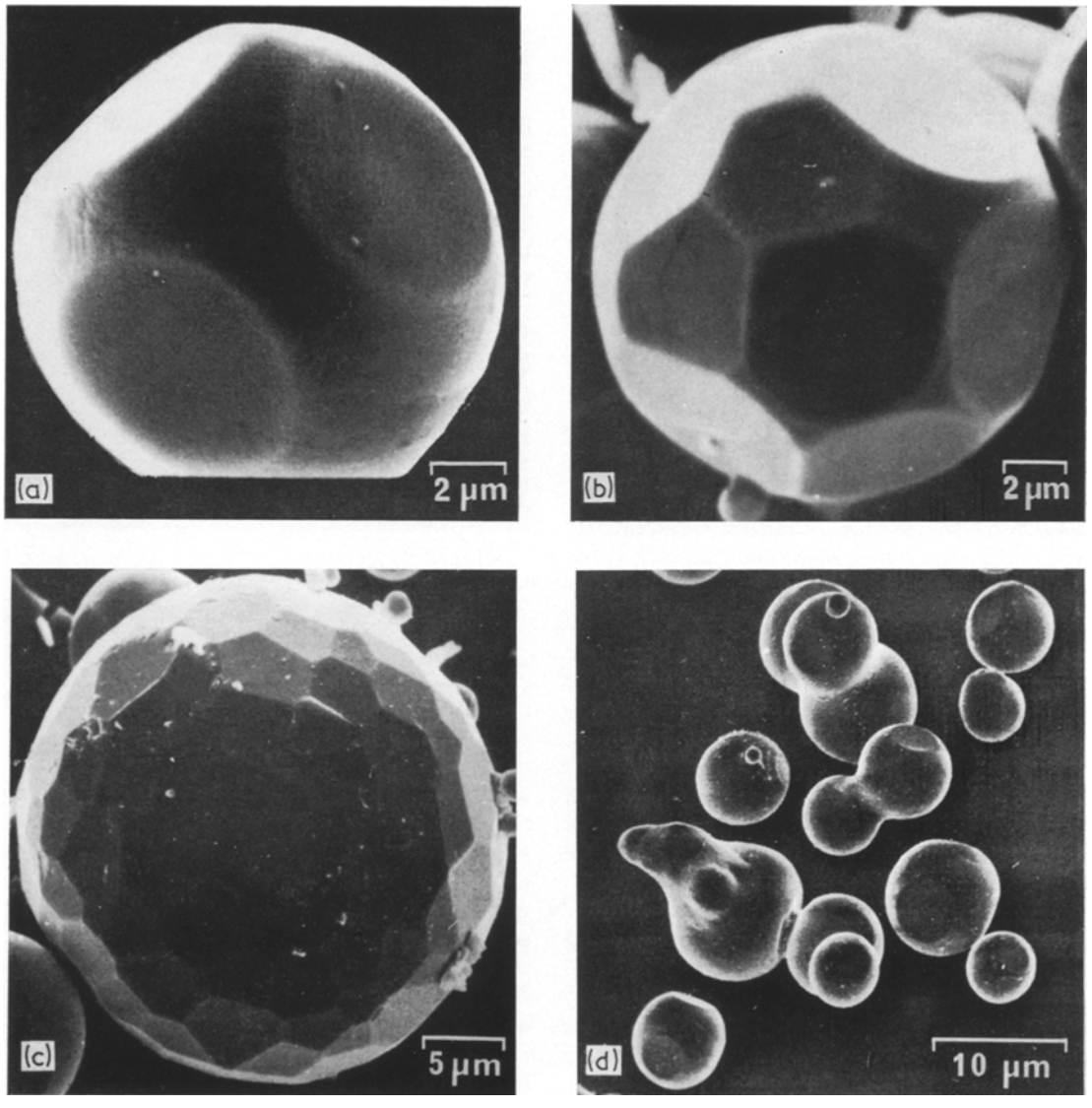

Figure 5 Spherical polycrystals. (a) Multi-dished sphere, (b) polyhedron with several unrelated faces, (c) multi-facetted sphere, (d) combined spheres.

diffraction were crystalline but the point at which the molten particles froze can only be inferred from indirect evidence. It was clear from micrographs that the positions of dishes, rings and other surface structures bore no relation to the attitudes of particles on the substrate. This shows that particles with these features developed them in the aerosol and must, therefore, have solidified in the aerosol.

The nature of the particles of Table II are now discussed by classes and then interrelated to give a qualitative picture of the processes that contribute to the formation of Cd aerosols.

4.1. Prismatic particles

4.1.1. General form and dendritic modification

From their geometry and symmetry the simple prisms are seen to be bounded when well formed by the basal $\{0001\}$ and prismatic $\{10\bar{1}0\}$ faces (Fig. 3). Pyramidal $\{10\bar{1}l\}$ faces are also seen on dendrites and on prisms of type *c* but the crystallographic relationship of the dendritic arms to

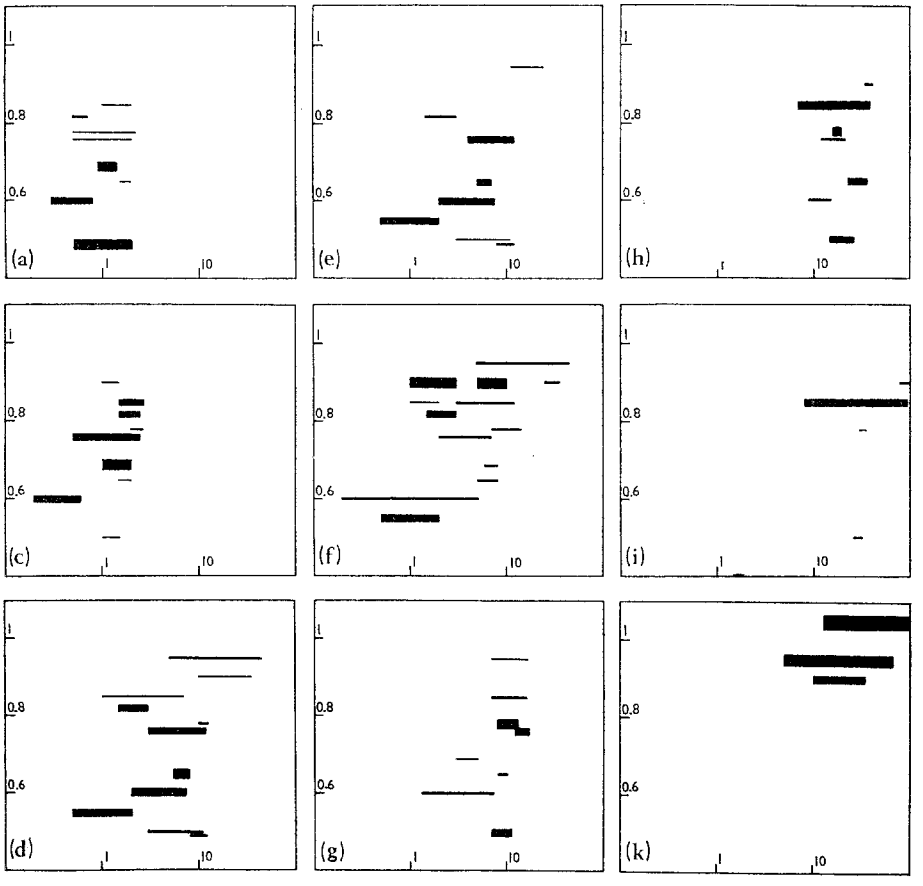

Figure 6 Morphological charts showing relation of diameter in μm (abscissa, log scale) and population fraction (linewidth) to dimensionless temperature T/T_f (ordinate) for particle types in Table I.

surfaces in Fig. 3a and d is not clear from micrographs. Arms appear to be incipient in the dentate protruberances of Fig. 3b, the typical skeletal particle.

The rarity with which simple prisms attain the smooth form of Fig. 3a or go over into a stellate dendrite (Fig. 3c) indicates that the latter two forms result from having grown respectively more slowly and more rapidly than the majority of particles of type *a*.

4.1.2. Skeletal modification

As distinct from the dishes on spheres, a hollow basal face would seem to be a frequent, though not invariable [8], feature of prisms of the cph metals that have undergone extensive growth in vapour diluted by a supporting gas. Nanev and Iwanov [9] observed the effect in the final forms of Cd and Zn crystals grown in mixtures of the vapour with H_2. Particles of about 1 mm diameter were obtained by first freezing a drop held on a cooled support and then growing it in the vapour to a prismatic monocrystal. The form of crystal resembled that in Fig. 3d although its base was not shown. A dish-shaped cavity formed in the upper basal face provided its diameter exceeded a certain size. On prolonged growth other faces developed signs of holes.

We have also seen crystals similar to those in Fig. 3b in the fall-out from Zn aerosols [10], and Van der Planken and Deruyttère [11] reported a circular indentation in the {0001} faces of Mg prisms grown accidentally in the vapour in the presence of Ar.

It has been proposed that the holes arise as a consequence of non-uniform conditions of supersaturation [9], it having been reasoned theoretically that above a certain size a polyhedral face cannot grow evenly under the control of diffusion in the surrounding medium [12-15].

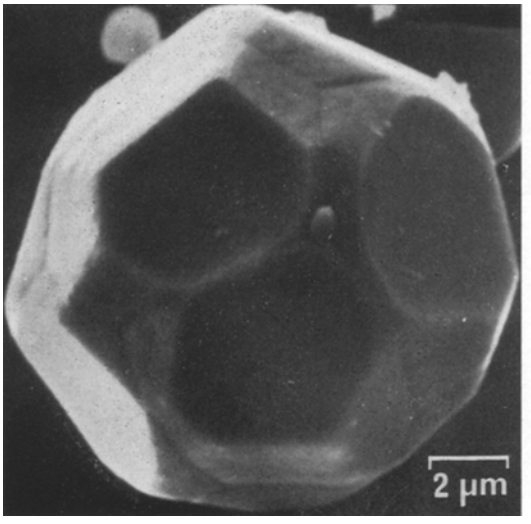

Figure 7 Multi-dished sphere with grooved boundaries.

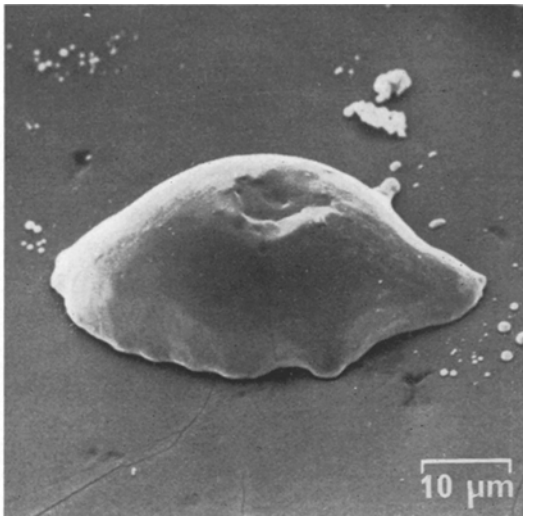

Figure 9 Splash.

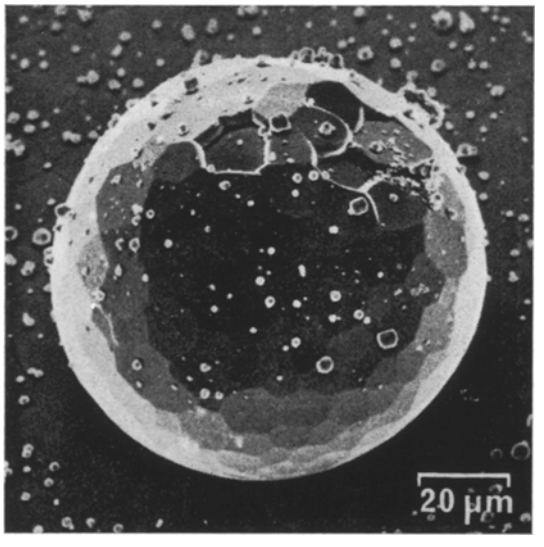

Figure 8 Multi-facetted sphere showing interior structure.

However, theoretical estimates of the critical size greatly exceeded those at which hollowing was actually seen [9].

4.2. Spheroidal particles

4.2.1. Monocrystals

In the case of spherical monocrystals the six-fold symmetry of the facets about an axis normal to the centre of the dish shows that its rim lies in the {0001} plane (Fig. 4). This conclusion enables the orientations of some of the facets to be determined by inspection. Electron micrographs (Fig. 4) and population charts (Fig. 6) show that a progressively smoother form is obtained on raising the temperature of the vapour to which the particle is exposed after birth in the cloudburst. As the basal dish is hardly affected by growth it is concluded that it is formed during solidification of the melt.

Circular flats, although not dishes, have frequently been observed on spheroidal monocrystals of Cd and Zn [8, 16-18]. Except in one case [18] the crystals examined were of millimeter size and were not aerosol particles but they showed many of the superficial features of our spherical monocrystals. The usual method of preparation was to freeze a molten particle to a crystal by cooling it on a surface under vacuum. In some work this crystal was used to provide the initial form for a study of vapour growth. The result of the cooling was often a monocrystal with the *c*-axis normal to the substrate, although a {0001} flat can develop in other orientations if the heat is not extracted through the substrate [16].

The mechanism of formation of the basal flat from a chance seed in a molten droplet is unknown. Mutaftschiev and Zell [18] in a study of the freezing of Cd drops reported that when the nucleus formed on the free surface of the melt the crystal first became visible as a flat, circular, basal raft from which the melt always withdrew at a finite contact angle. They concluded that the

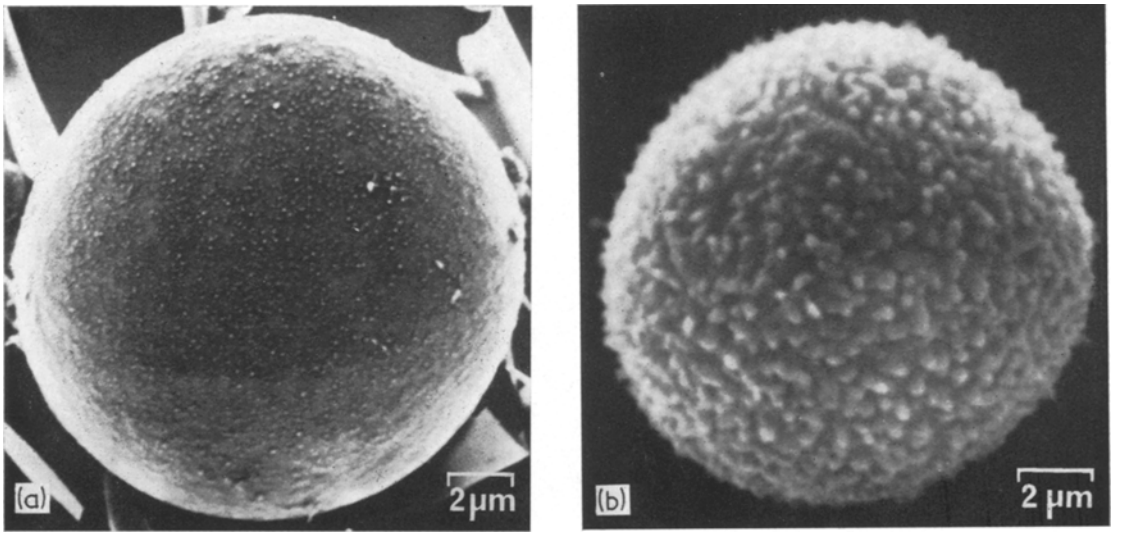

Figure 10 Smooth sphere (a) as normally seen and (b) after exposure to air.

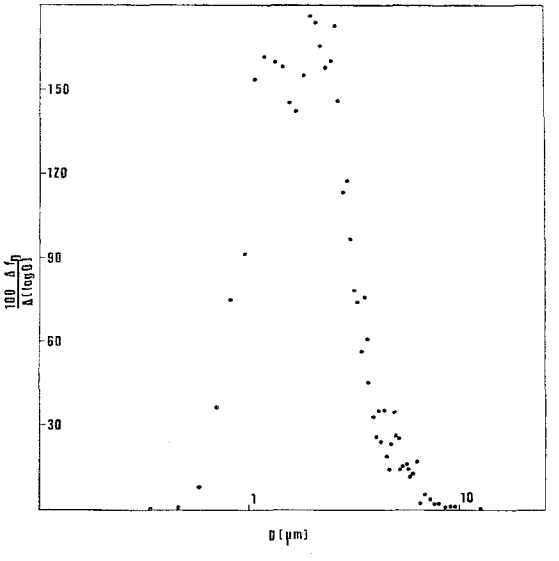

Figure 11 Size distribution of particles (all types) in fall-out at 0.76 T_f.

flat must have formed by a lateral growth mechanism under the liquid surface and not by nucleation and growth of layers on the face. It was not explained how the growth front advanced into the interior to complete solidification. Heyer *et al.* [16] also reported that a circular {0001} face was first to appear and that it was quite smooth.

As the shallow cavities seen by Nanev and Iwanov developed after solidification, there would appear to be a relationship between our dishes and melt-grown flats. Our particles have also grown further after solidification so that cavitation of the basal flat indicates a special difficulty of growth upon it. As to the nature of this inhibition, alternatives may be envisaged to the vapour starvation theory put forward by Nanev and Iwanov. The possibility of contamination in the present study was suggested by the observation in early preparations of dishes studded with protrusions of a powdery substance resembling the amorphous material in Fig. 10b. This was no longer found on dished particles upon using a substantially improved vacuum for the coating process, and it was probably the result of oxidation through an imperfect Au–Pd film. Kimoto and Nishida [4] found that traces of air in the vacuum chamber had deleterious effects on the crystallinity of condensed particles. In their case particles were condensed in the vacuum chamber and removed for examination without protection.

To affect the growth of particles, the contaminant would have to be present inside the cloud chamber. Indigenous impurity could be responsible for the formation of the basal flat in the melt as well as for its tendency to persist afterwards. Chernov [15, 19] suggested that impurity, not vapour diffusion, might explain the cavities of Nanev and Iwanov, and reaction with residual oxygen is believed to interfere with the

free evaporation of metal from {0001} faces of Zn crystals although apparently not affecting $\{10\bar{1}0\}$ faces [20].

Features of spherical monocrystals that are eradicated by vapour growth at high temperatures are the facets and rings. Fig. 4 shows that rings originate as the edges of growth terraces making up the flat, pyramidal faces $\{10\bar{1}l\}$ between the basal plane and the prismatic planes that surround the hexagonal axis. Last to disappear are the rings of small circumference which lie on planes of low l index. Their final form is circular and indicative of the tendency towards isotropy of the edge free-enthalpy. Alternating with the flat pyramids around the axis are pyramids of a second kind. These are rough and cavitated at low temperature (Fig. 4b). Alternation of smooth and rough pyramids has frequently been observed on macroscopic crystals, and the coarse texture is promoted by low temperatures and low supersaturations [16, 21]. It is not known in the present case if, due to differences in growth rates that existed in the droplet, the crystal begins vapour growth in the form of Fig. 4b or whether roughness develops after solidification.

Rounding-off of the hemisphere opposite the basal dish is apparently unimpeded, so that poisoning of the vapour growth mechanism does not operate on this side. Apart from the dish the particle is bilaterally symmetrical (Fig. 4) and it is possible that the floor of the basal dish represents the terminus of the crystallization front which advanced steadily across the droplet from a nucleus on the surface, sweeping soluble, involatile impurity before it in a natural zone-refining operation. This interpretation would appear to conflict with the view of Mutaftschiev and Zell but is in keeping with the presence of an impurity that affects only the subsequent vapour growth.

Evidence from other studies on condensation aerosols is far from plentiful. Movilliat [22] obtained spheroidal Cd particles of 0.5 μm diameter by the boiler method with N_2 as carrier gas. There was slight indication of orientated faces but the particles were seriously affected by oxidation. The spherical particles of Van der Planken and Deruyttère, which may have condensed as aerosols, showed no evidence of crystal planes and appear to have been heavily contaminated. Sub-micron Zn particles were obtained by Bauer [23] who quenched Zn–Ar flows with cold Ar, and McBride and Sherman's supersonic expansions of Zn–He gave particles of Zn which they reported to be close to spherical in shape although only about 10 nm in diameter [24]. The transmission electron micrographs of Kimoto and associates [3, 4], and of Wada [25], were of low-pressure condensates and are unfortunately of limited use in the diagnosis of the growth sequences, but it was shown that the particle size tends to increase with the pressure of supporting gas and with its atomic weight (He, Ar, Xe). This may reflect the increased time that particles remained suspended in the vapour in their low-pressure environments.

4.2.2. Polycrystals

The particles of Fig. 5a and b appear to differ mainly in the number of faces. Their limited size in comparison with smooth spheres (Fig. 6), and the absence of rough faces, is consistent with the view that at least some of the faces are basal dishes. Their orientations and the absence of tree rings would be explained by the radial advance of crystallization fronts from nuclei at the centre of the droplet.

The example of Fig. 7 was apparently a multi-dished sphere which assumed polyhedral form after a limited amount of growth in the vapour, since boundaries have become visible as grooves at the intersections of pyramidal facets. This observation establishes an important connection between the multi-dished sphere and the polyhedral particle (Table I, g, h). If all the faces on a polyhedron were basal dishes it would be expected to remain smaller than a sphere because of difficulty of growth. Fig. 6 shows the opposite to be true, and it is suspected that the polyhedra of Figs. 5b and 7 are enclosed by both dishes and pyramidal facets. Fig. 7 would then represent an intermediate form in the conversion of a multi-dished sphere to a polyhedron, the pyramids having been in the process of merging to form new polygonal faces. These are sometimes not easy to distinguish from dishes which have acquired one or more straight edges by impingement on other dishes (Fig. 7). Growth in the vapour involves condensation on areas between the basal dishes, and while it continues it accentuates their curvature.

It is significant that the multi-faceted particle of Fig. 8 has other aerosol particles attached to it. Many of them have diameters smaller than the thickness of the faceted layer, so that this could only be a Cd layer: the Au–Pd was applied after the aerosol had settled. The uniform

appearance of the Cd layer indicates formation before the particle came to rest. The damage in Fig. 8 would then be explained by impact with the substrate rather than a handling accident especially as there is aerosol sediment on the surface exposed by the broken layer.

The layer has ruptured apparently along the grain boundaries between the crystals composing it. The presence of these crystals if due to vapour growth, might be expected to depend on the lowering of the barriers to random nucleation and growth on a smooth host particle. Conditions favourable to this would be found only on particles condensed at temperatures approaching T_s, the lowest freezing point of supercooled droplets. On such grounds the position of T_s could be placed within 0.8 T_f to 0.9 T_f (Fig. 6). It is still unclear how the core of the particle attains such a size at these temperatures.

Replacement of dished spheres by smooth ones occurs in the same range, 0.8 T_f to 0.9 T_f, and is believed to indicate a change in the mechanism of solidification. This is likely on account of the absence of basal faces on the new particles. The lack of any obvious differences in smooth spheres produced above and below T_f may be adduced as evidence of supercooling, the particles always solidifying on the substrate during withdrawal from the furnace. This would explain the absence of particles frozen into attitudes of distortion by impact with the substrate. It would also be consistent with the bodily shift in the size range of smooth spheres as the temperature passes T_f (Fig. 6).

Present evidence does not show whether the change from dished to smooth spheres is abrupt as would be expected if it took place at the threshold of spontaneous freezing, T_s. Only if the growth of the crystalline nucleus is sufficiently rapid will the onset of nucleation be apparent in a sudden change from liquid to solid fall-out. A similar problem in locating T_s occurred with the halides of the heavy metals [7], where flattening of particles on impact with the substrate although extensive was not sensitively temperature-dependent.

4.3. Origin and development of aerosol particles

In this work the growth features associated with the unique *c*-axis of the Cd lattice are an important guide to the crystal morphology and growth mechanisms. The variety of particles produced in a cloudburst shows that several mechanisms can operate simultaneously but as yet we have no information on the rates. The numbers of particles cannot be judged from Fig. 6 but it does show that the final forms are correlated with the steady wall temperature, T, rather than with the way the supersaturator is operated to induce condensation initially. It is therefore concluded that heat transfer to the walls plays a dominant role in the final stages of particle development. The uniqueness of prisms, which do not respond to increase of temperature by growth in the way that spherical particles do, raises the possibility that, as previously suspected of the dendritic particles in salt aerosols [7], the difference originates at the nucleation stage, prismatic crystals self-nucleating as solid while spherical forms condense first to the melt.

Acknowledgement

We are grateful to S.R.C. for support including a maintenance award to K.C.P.

References

1. E. R. BUCKLE and K. C. POINTON, *J. Chem. Soc. Faraday Symp.* **7** (1973) 78.
2. M. S. GEN, M. S. ZISKIN and YU. I. PETROV, *Dokl. Akad. Nauk SSSR* **127** (1959) 366.
3. K. KIMOTO, Y. KAMIYA, N. NONOYAMA and R. UYEDA, *Jap. J. Appl. Phys.* **2** (1963) 702.
4. K. KIMOTO and I. NISHIDA, *ibid* **6** (1967) 1047.
5. L. HOLLAND, "Vacuum Deposition of Thin Films" (Chapman and Hall, London, 1956).
6. D. G. DRUMMOND, *J. Roy. Microsc. Soc.* **70** (1950) 1.
7. E. R. BUCKLE and C. N. HOOKER, *Trans. Faraday Soc.* **58** (1962) 1939.
8. R. KAISHEV and C. NANEV, "Growth of Crystals", edited by N. N. Sheftal (Proc. Symp. Crystal Growth, Moscow, 1966) p. 19.
9. C. NANEV and D. IWANOV, *J. Crystal Growth* **4** (1968) 530.
10. E. R. BUCKLE and K. C. POINTON, *J. Chem. Soc. Faraday Symp.* **7** (1973) 97.
11. J. VAN DER PLANKEN and A. DERUYTTÈRE, *J. Crystal Growth* **11** (1971) 273.
12. A. SEEGER, *Phil. Mag.* **44** (1953) 1.
13. A. A. CHERNOV, *Kristallografiya* **7** (1962) 895.
14. *Idem, ibid* **8** (1963) 87.
15. *Idem, ibid* **16** (1971) 842.
16. H. HEYER, F. NIETRUCH and I. N. STRANSKI, *J. Crystal Growth* **11** (1971) 283.
17. R. KAISHEV and C. NANEV, *Phys. Stat. Sol.* **10** (1965) 779.
18. B. MUTAFTSCHIEV and J. ZELL, *Surface Sci.* **12** (1968) 317.
19. A. A. CHERNOV, in [9] p. 534.
20. R. W. MAR and A. W. SEARCY, *J. Chem. Phys.* **53** (1970) 3076.

21. C. NANEV, *Phys. Stat. Sol.* **16** (1966) 777.
22. P. MOVILLIAT, *Ann. Occup. Hyg.* **4** (1962) 275.
23. H. E. BAUER, Rept. K-910900-9, United Aircraft Research Laboratories, East Hartford, Conn., September 1971.
24. D. D. MCBRIDE and PAULINE M. SHERMAN, *AIAA Journal* **10** (1972) 1058.
25. N. WADA, *Jap. J. Appl. Phys.* **7** (1968) 1287.

Received 9 May and accepted 5 July 1974.